UCSF
UC San Francisco Previously Published Works

Title

Inhibition of RNA lariat debranching enzyme suppresses TDP-43 toxicity in ALS disease models

Permalink

https://escholarship.org/uc/item/3wp211gh

Journal

Nature Genetics, 44(12)

ISSN

1061-4036

Authors

Armakola, Maria
Higgins, Matthew J
Figley, Matthew D
et al.

Publication Date

2012-12-01

DOI

10.1038/ng.2434

Peer reviewed

eScholarship.org Powered by the California Digital Library
University of California

Author Manuscript

Author Manuscript

Author Manuscript

Author Manuscript

HHS Public Access

Author manuscript

Nat Genet. Author manuscript; available in PMC 2013 June 01.

Published in final edited form as:

Nat Genet. 2012 December ; 44(12): 1302–1309. doi:10.1038/ng.2434.

Inhibition of RNA lariat debranching enzyme suppresses TDP-43 toxicity in ALS disease models

Maria Armakola[1,2,10], **Matthew J. Higgins**[3,10], **Matthew D. Figley**[1], **Sami J. Barmada**[4], **Emily A. Scarborough**[5], **Zamia Diaz**[5], **Xiaodong Fang**[1], **James Shorter**[5], **Nevan J. Krogan**[3,6,7], **Steven Finkbeiner**[4], **Robert V. Farese Jr.**[3,8,9,11], and **Aaron D. Gitler**[1,11]

Robert V. Farese: bfarese@gladstone.ucsf.edu; Aaron D. Gitler: agitler@stanford.edu

[1]Department of Genetics, Stanford University School of Medicine, Stanford, CA 94305

[2]Neuroscience Graduate Group, Perelman School of Medicine at the University of Pennsylvania, Philadelphia, PA 19104 USA

[3]Gladstone Institute of Cardiovascular Disease, Taube-Koret Center, Hellman Family Foundation Program, J. David Gladstone Institutes, San Francisco, CA 94158 USA

[4]Gladstone Institute of Neurological Disease, Taube-Koret Center, Hellman Family Foundation Program, J. David Gladstone Institutes, San Francisco, CA 94158 USA

[5]Department of Biochemistry and Biophysics, Perelman School of Medicine at the University of Pennsylvania, Philadelphia, PA 19104 USA

[6]Department of Cellular and Molecular Pharmacology, University of California, San Francisco, CA 94158 USA

[7]California Institute for Quantitative Biosciences, QB3, San Francisco, CA 94158 USA

[8]Department of Medicine, University of California, San Francisco, CA 94158 USA

[9]Department of Biochemistry & Biophysics, University of California, San Francisco, CA 94158 USA

Abstract

ALS is a devastating neurodegenerative disease primarily affecting motor neurons. Mutations in TDP-43 cause some forms of the disease, and cytoplasmic TDP-43 aggregates accumulate in degenerating neurons of most ALS patients. Thus, strategies aimed at targeting the toxicity of

Users may view, print, copy, download and text and data- mine the content in such documents, for the purposes of academic research, subject always to the full Conditions of use: http://www.nature.com/authors/editorial_policies/license.html#terms

[11]Correspondence should be addressed to: Aaron D. Gitler, 300 Pasteur Drive, M322 Alway Building, Stanford, CA 94305, 650-725-6991 (phone), 650-725-1534 (fax). Robert V. Farese, Jr., Gladstone Institute of Cardiovascular Disease, 1650 Owens Street, San Francisco, CA 94158, 415-734-2714 (phone), 415-355-0960 (fax).

[10]These authors contributed equally to this work.

AUTHOR CONTRIBUTIONS

M.A., M.J.H., M.D.F., S.J.B., J.S., N.J.K., S.F., R.V.F., and A.D.G. designed the experiments. M.A., M.J.H., M.D.F., S.J.B., J.S., E.A.S., Z.D., X.F., and A.D.G. performed the research. M.A., M.J.H., M.D.F., S.J.B., J.S., N.J.K., S.F., R.V.F., and A.D.G. analyzed and interpreted data. M.A., M.J.H., M.D.F., S.J.B., S.F., R.V.F., and A.D.G. wrote the paper with contributions from all authors.

COMPETING FINANCIAL INTERESTS

A.D.G. is an inventor on patents and patent applications that have been licensed to FoldRx.

Author Manuscript Author Manuscript Author Manuscript Author Manuscript

cytoplasmic TDP-43 aggregates may be effective. Here we report results from two genome-wide loss-of-function TDP-43 toxicity suppressor screens in yeast. The strongest suppressor of TDP-43 toxicity was deletion of Dbr1, which encodes RNA lariat debranching enzyme. We show that in the absence of Dbr1 enzymatic activity intronic lariats accumulate in the cytoplasm and likely act as decoys to sequester TDP-43 away from interfering with essential cellular RNAs and RNA-binding proteins. Knockdown of Dbr1 in a human neuronal cell line or in primary rodent neurons is also sufficient to rescue TDP-43 toxicity. Our findings provide insight into TDP-43 cytotoxicity and suggest decreasing Dbr1 activity could be a potential therapeutic approach for ALS.

INTRODUCTION

Amyotrophic lateral sclerosis (ALS), also known as Lou Gehrig's disease, is a late-onset neurodegenerative disease characterized by loss of motor neurons, progressive weakness and eventually paralysis and death within 3–5 years[1]. Most ALS cases are sporadic (SALS), but 10% are familial (FALS), of which ~20% result from mutations in the Cu/Zn superoxide dismutase 1 gene (SOD1)[2]. SOD1 mutations are thought to cause disease by a toxic gain-of-function[3], and thus, strategies to lower SOD1 levels are being pursued[4]. However, SOD1 mutations account for only a small percentage of ALS cases. Additional therapeutic strategies are needed.

RNA-binding proteins and RNA-processing pathways have recently been implicated in ALS[5,6]. The RNA-binding protein TDP-43 was found in cytoplasmic inclusions in spinal cord neurons of most non-SOD1 ALS cases[7,8] and mutations in TDP-43 were identified in FALS and SALS cases[9–13]. Mutations in another RNA-binding protein, FUS/TLS, were also found in some ALS patients[14–18]. Therefore, therapies targeting TDP-43 and/or FUS could be effective in cases not caused by SOD1 mutations. Interestingly, TDP-43 inclusions occur in many frontotemporal dementia cases, including, and targeting TDP-43 may be effective for these patients. Efforts are underway to define the mechanisms by which TDP-43 and FUS and defects in RNA processing pathways contribute to ALS.

We have used yeast models to illuminate mechanisms underpinning TDP-43 and FUS aggregation and cellular toxicity[19–21]. TDP-43 forms aggregates in the cytoplasm of yeast cells and is toxic, recapitulating two key features of TDP-43 relevant to human disease[19]. We used a genome-wide plasmid overexpression screen to identify modifiers of aggregation and toxicity. One modifier of toxicity was Pbp1, whose human homolog, ataxin 2, harbors a polyglutamine tract that is expanded (>34 glutamines) in spinocerebellar ataxia type 2. We found that intermediate-length polyQ expansions (~27–33 glutamines) in ataxin 2 are a significant genetic risk factor for ALS[22,23]. Additional genetic modifiers of TDP-43 toxicity in yeast might provide more insight into pathogenic mechanisms and could represent novel therapeutic targets.

Here we report results from a genome-wide loss-of-function screen to identify yeast genes that modify TDP-43 toxicity. In our previous screen ([22] and A.D.G. unpublished), we used a library of yeast overexpression plasmids. Here, we interrogated collections of non-essential yeast knockouts and knockdowns of essential genes. Loss-of-function screens may be useful to identify therapeutic targets for which inhibitors could be developed. Among the most

Author Manuscript Author Manuscript Author Manuscript Author Manuscript

potent knockout suppressors of TDP-43 toxicity was *dbr1*Δ. Dbr1 catalyzes the debranching of lariat introns that are formed during pre-mRNA splicing. We show that inhibiting Dbr1's debranching enzymatic activity is sufficient to rescue TDP-43 toxicity. We further provide evidence that intronic lariat species that accumulate in the cytoplasm of *dbr1*Δ cells act as decoys to sequester toxic cytoplasmic TDP-43, possibly preventing it from interfering with other essential cellular RNA targets and other RNA-binding proteins. Knockdown of Dbr1 in a human neuronal cell line and in primary rodent neurons is also sufficient to rescue TDP-43 toxicity, suggesting that the effect of Dbr1 on TDP-43 toxicity is conserved from yeast to mammals. We propose that the debranching enzymatic activity of Dbr1 could be a potential therapeutic target for ALS and related TDP-43 proteinopathies.

RESULTS

Identification of Dbr1 as a potent modifier of TDP-43 toxicity in yeast

To identify genes that modify TDP-43 toxicity, two independent unbiased genome-wide yeast deletion screens were performed in two laboratories (Supplementary Fig. 1). Similar approaches have been used to discover modifiers of neurodegenerative disease proteins α-synuclein, huntingtin, and FUS/TLS[21,24,25]. In the first screen, we used synthetic genetic array (SGA) analysis[26] to introduce a galactose-inducible TDP-43 expression plasmid into each non-essential yeast deletion strain by mating (Supplementary Fig. 1a). The second screen included the deletion genes and a library of essential genes generated by decreased abundance by mRNA perturbation (DAmP) technology[27] (Supplementary Fig. 1 b–e). We selected yeast deletion strains in which TDP-43 was more (enhancer) or less (suppressor) toxic than in wild-type (WT) cells. Screen 1 was repeated three independent times and only hits that were reproduced all three times were selected. Screen 2 contained three biological and two technical replicates (six replicates total), which allowed the calculation of an interaction score. To provide independent evidence that the gene deletions identified from the screens modify TDP-43 toxicity, we generated gene deletions for the hits from screen 1 and selected genes from screen 2 in an independent strain background and confirmed the effects on TDP-43 toxicity. In screen 1, we identified 14 yeast deletion strains that modified TDP-43 toxicity (Table 1), six enhancers and eight suppressors. The more sensitive and quantitative analysis of screen 2 allowed us to identify a total of 2,581 potential enhancers and 2,056 potential suppressors (Supplementary Data Set 1). In analyzing these results, we chose to focus here on suppressors of TDP-43 toxicity because these could represent attractive therapeutic targets for small molecule inhibitors or RNA interference (see Supplementary Note for discussion of additional yeast TDP-43 toxicity modifier genes).

One of the most effective deletion suppressors of TDP-43 toxicity identified independently in both screens was *dbr1*Δ, and we focused further efforts on it. Dbr1 deletion suppressed the toxicity of WT TDP-43 as well as an ALS-linked mutant form of TDP-43 (Q331K, Fig. 1a and Supplementary Fig. 2). Immunoblotting confirmed that toxicity was not suppressed because of decreased TDP-43 expression in the *dbr1*Δ strain (Fig. 1b). Deletion of Dbr1 did not suppress the toxicity of two other neurodegenerative disease proteins, α-synuclein and mutant huntingtin. Indeed, huntingtin toxicity was slightly enhanced in the *dbr1*Δ strain (Fig. 1a). However, Dbr1 deletion suppressed toxicity of another RNA-binding protein

Author Manuscript Author Manuscript Author Manuscript Author Manuscript

linked to ALS, FUS/TLS (Fig. 1a), demonstrating specificity of the Dbr1 genetic interaction for ALS-linked RNA-binding proteins TDP-43 and FUS/TLS.

Inhibiting Dbr1 suppresses TDP-43 toxicity in mammalian cells

Identification of Dbr1 as a potent modifier of TDP-43 toxicity suggests the possibility that inhibiting Dbr1 enzymatic activity (Fig. 1c) could be a promising therapeutic strategy for ALS, especially since TDP-43 is thought to contribute broadly to almost all non-SOD1 ALS cases[7]. Therefore, we tested if inhibiting Dbr1 function could rescue TDP-43 toxicity in mammalian cells. We generated a stable human M17 neuroblastoma cell line that inducibly expresses epitope-tagged ALS-linked mutant TDP-43 (Q331K), under control of a doxycycline-regulated promoter (Fig. 2a). Inducible expression of TDP-43 Q331K was confirmed by immunofluorescence and immunoblotting (Fig. 2b and data not shown). Upregulating mutant TDP-43 was toxic in these cells (Fig. 2c). To determine if inhibiting Dbr1 rescues TDP-43 toxicity, we transfected these cell lines with an siRNA against human *DBR1* or a non-targeting control siRNA (Fig. 2d). Neither siRNA affected TDP-43 expression levels in these cells (data not shown). Whereas the non-targeting siRNA had no effect on toxicity, transfection with the *DBR1*-specific siRNA significantly reduced TDP-43 toxicity (Fig. 2d).

Inhibiting Dbr1 suppresses TDP-43 toxicity in primary neurons

We next asked whether knockdown of Dbr1 prevents TDP-43-mediated toxicity in primary neurons. We showed previously that overexpression of TDP-43 in primary cortical neurons induces neurodegeneration with cytoplasmic mislocalization and aggregation of TDP-43, recapitulating several key pathologic features of TDP-43 proteinopathies *in vitro*[28]. To determine if Dbr1 knockdown protects neurons from TDP-43 cytotoxicity, we used automated microscopy and longitudinal analysis, a technique that identifies and characterizes variables that significantly contribute to neuronal survival[29]. We isolated and cultured rodent primary cortical neurons and transfected them with three constructs: (1) mApple, (2) enhanced green fluorescent protein (EGFP) or TDP-43 fused to EGFP (TDP-43-EGFP), and (3) siRNA directed against Dbr1 (sR-Dbr1) or scrambled siRNA (sR-Sc). With automated microscopy, hundreds of individual neurons were imaged from each cohort at regular, 24-hr intervals for 8 days (Fig. 3a). In this case, mApple serves as a sensitive survival marker, since the loss of mApple fluorescence, cell blebbing, or disruption of the cell membrane signifies cell death[29]. These criteria are at least as specific as traditional markers of particular cell death pathways, but have the advantage of detecting all forms of cell death in a single assay and are therefore more sensitive. Because each neuron in a population can be followed longitudinally for an extended period of time, the analysis is analogous to that used in a prospective clinical trial. Powerful statistical tools developed for human epidemiological studies, including Kaplan-Meier survival analysis and Cox proportional hazards analysis, are used to describe the data that are generated from these experiments.

We initially performed a small pilot experiment to determine the optimal amount of Dbr1 siRNA (Supplementary Fig. 3), and found that the most effective dose was 30 nM Dbr1 siRNA. Based on the effect size that we noted in the pilot experiment, subsequent

Author Manuscript Author Manuscript Author Manuscript Author Manuscript

experiments were scaled to a population size to achieve the power necessary to detect a significant effect on neuronal survival. As expected, the risk of death in primary cortical neurons was significantly greater in neurons expressing TDP-43-EGFP than in control neurons expressing EGFP alone (Fig. 3b). The relative risk or hazard ratio (HR) calculated by Cox proportional hazards analysis was 2.23 ($p < 1\times10^{-9}$), signifying an approximately twofold increase in the risk of death. Knockdown of Dbr1 in neurons expressing TDP-43-EGFP reduced the risk of death by nearly 20%, with an HR of 0.81 (p 0.04). In contrast, knocking down Dbr1 had no effect upon the survival of the control cohort expressing EGFP alone (HR 1.2, p 0.3). Using a Kaplan-Meier survival curve to display the same data demonstrates a similar effect on neuron survival (Fig. 3c). Interestingly, this improvement in survival did not depend on decreased cytoplasmic TDP-43. In fact, we observed significantly more primary neurons with cytoplasmic TDP-43 when treated with Dbr1 siRNA than with control siRNA (Fig. 3d). These data suggest that neurons can survive even in the face of cytoplasmic TDP-43. These results in primary neurons expressing human TDP-43 extend the protective effect of Dbr1 knockdown that we observed in yeast and in neuroblastoma cells, and indicate that the ability of Dbr1 inhibition to suppress the toxic effects of TDP-43 accumulation is conserved from yeast to mammalian cells, organisms separated by a billion years of evolution.

Dbr1 lariat debranching enzymatic activity is required for TDP-43 toxicity

DBR1 encodes an RNA debranching enzyme, highly conserved from yeast to man, that cleaves the 2′-5′ phosphodiester bonds of lariat introns that are formed during pre-mRNA splicing[30,31] (Fig. 1c). After transcription, primary pre-mRNA transcripts are processed by the spliceosome to remove introns, which are released as lariats[32]. Lariats are formed during splicing when the 5′-exon attacks the 3′-splice site in a nucleophilic manner. RNA nucleases within the cell can digest the 3′ tail of the lariat introns but the lariat structure is resistant to digestion until Dbr1, a specialized debranching enzyme, cleaves the 2′-hydroxyl-5′-phosphate bond (Fig. 1c). Thus, debranching appears to be a rate-limiting step for the turnover of intronic RNA because the steady-state levels of lariat introns are greatly increased in *dbr1*Δ cells[31,33].

Deletion of Dbr1 reduced TDP-43 toxicity in yeast (Fig. 1), mammalian cells (Fig. 2) and primary neurons (Fig. 3), but it was unclear whether the rescue was because of loss of debranching enzymatic activity or potentially another Dbr1 function. To test this directly, we used “debranching activity dead” mutants of Dbr1. We co-transformed *dbr1*Δ cells with expression plasmids for TDP-43 and either WT Dbr1 or two independent Dbr1 point mutants (D40A or N85A) that lack debranching enzymatic activity *in vitro* and *in vivo*[33]. Immunoblotting confirmed that the WT and mutant Dbr1 proteins were expressed at equivalent levels (Fig. 4a). Whereas expressing WT Dbr1 restored TDP-43 toxicity to *dbr1*Δ cells, expressing either of the debranching-inactive Dbr1 point mutants did not (Fig. 4b). Moreover, we tested a panel of 16 Dbr1 mutants, some of which retain full debranching activity others that have lost all activity, and others with partial debranching activity[33]. There was a perfect correlation between debranching activity and ability to restore TDP-43 toxicity to *dbr1*Δ cells: WT Dbr1 fully restored TDP-43 toxicity, whereas completely inactive Dbr1 had no effect, and partially active Dbr1 partially restored TDP-43 toxicity

Author Manuscript Author Manuscript Author Manuscript Author Manuscript

(Supplementary Table 1). Thus, inhibiting Dbr1 debranching enzymatic activity is sufficient to rescue TDP-43 toxicity in yeast cells. Finally, expressing mammalian Dbr1 (mDbr1) in *dbr1*Δ cells was also sufficient to restore TDP-43 toxicity (Fig. 4b), indicating the debranching function of Dbr1 is conserved from yeast to mammals.

TDP-43 toxicity suppression is mediated by lariat intron accumulation

In the absence of Dbr1, steady-state levels of lariat introns are greatly increased [33]. This suggested an intriguing possibility. Perhaps the accumulating lariat introns in *dbr1*Δ cells act as a kind of decoy for TDP-43, sequestering it away from important cellular RNAs and other RNA-binding proteins. First, we determined if the rescue of TDP-43 toxicity was specific to lariat intron accumulation or if accumulation of any non-specific RNA species rescued toxicity. We expressed TDP-43 in three other yeast deletion strains, *upf1*Δ, *upf2*Δ, and *xrn1*Δ, that each result in accumulation of RNA species within the cell owing to alterations in the nonsense-mediated decay (NMD) pathway[34–38]. Whereas, deleting Dbr1 rescued TDP-43 toxicity, TDP-43 toxicity was not suppressed in *upf1*Δ, *upf2*Δ, or *xrn1*Δ cells and was even slightly enhanced in *upf1*Δ and *upf2*Δ cells (Fig. 4c), suggesting that the rescue of TDP-43 toxicity is specific to intronic lariat accumulation.

Intronic lariats in *dbr1*Δ cells act in the cytoplasm to suppress TDP-43 toxicity

We next sought to determine the mechanism by which intronic lariats suppress TDP-43 toxicity in *dbr1*Δ cells. We and others showed TDP-43 is toxic in the cytoplasm in multiple cellular and animal model systems[19,28,39,40]. Perhaps intronic lariats accumulate in the nucleus of *dbr1*Δ cells, sequester TDP-43 there and prevent it from aggregating in the cytoplasm, and thereby suppress toxicity. In this model, sequestering TDP-43 in the cytoplasm should overcome the toxicity suppression by *dbr1*Δ. To test this, we retained TDP-43 in the cytoplasm by mutating the nuclear localization signal (NLS)[22,41]. We reasoned that, if *dbr1*Δ suppresses TDP-43 toxicity in the nucleus, the ΔNLS mutant TDP-43 ould still be toxic. Surprisingly, Dbr1 deletion still suppressed toxicity when TDP-43 was sequestered in the cytoplasm (Fig. 5a), suggesting the site of action of intronic lariats is the cytoplasm.

The above genetic result suggested that intronic lariats act in the cytoplasm to suppress TDP-43 toxicity. To test this directly, we developed a method to visualize, in living cells, the endogenous intronic lariats that accumulate in *dbr1*Δ cells. We reasoned that, if we could visualize the intronic lariats, we could determine 1) if they localized to the cytoplasm or nucleus and 2) if they co-localized with TDP-43 inclusions. A technique to visualize the localization of endogenous mRNAs in living yeast cells was recently developed[42]. m-TAG uses homologous recombination to insert binding sites for the RNA-binding MS2 coat protein (MS2-CP) between the coding region and 3′UTR of any yeast gene. Expression of MS2-CP fused to GFP enables the visualization of any yeast mRNA that has been tagged with MS2 binding sites[42–44]. We modified m-TAG to visualize intronic lariats. Instead of tagging the 3′UTR of a target yeast gene, we used homologous recombination to integrate MS2 binding sites in the intron of the *ACT1* gene (Fig. 5b), which has previously been shown by northern blot analysis to accumulate in the absence of Dbr1 activity[33].

Author Manuscript Author Manuscript Author Manuscript Author Manuscript

We transformed WT and *dbr1*Δ yeast cells, each harboring MS2 binding sites integrated in the intron of the *ACT1* gene (Fig. 5c), with a plasmid containing a 3XGFP-tagged MS2-CP RNA-binding protein under control of the inducible *MET25* promoter. We analyzed the localization of MS2-CP-GFP by fluorescence microscopy. As reported[43], because the *MET25* promoter is somewhat leaky, we detected the GFP fusion protein even without induction (by growth in the presence of methionine). In WT cells, in which no intronic lariats should accumulate[33], we detected faint MS2-CP-GFP expression in a diffuse pattern throughout the cell (Figs. 5c and Supplementary Fig. 4). In contrast, in *dbr1*Δ cells, MS2-CP-GFP accumulated in one or two bright foci per cell and these were always located in the cytoplasm (Fig. 5c). We observed similar results by tagging an independent intron from another yeast gene, *CYH2* (data not shown). These foci could represent the excised lariat introns that accumulate in *dbr1*Δ cells or a splicing intermediate[45] (also see Supplementary Note). However, since we did not see them in WT cells in which *ACT1* or *CYH2* introns were tagged with MS2 sequences (Figs. 5c and Supplementary Fig. 4), these foci are likely to be lariat introns that accumulate in the absence of Dbr1 activity.

Intronic lariats colocalize with TDP-43 cytoplasmic foci in yeast

Having established that intronic lariats accumulate in the cytoplasm of *dbr1*Δ cells, we next tested our hypothesis that the accumulating lariats in *dbr1*Δ cells act as a decoy for TDP-43 by preventing it from interacting with other important cellular RNAs and RNA-binding proteins. We expressed untagged TDP-43 in WT and *dbr1*Δ cells and visualized its localization by immunocytochemistry with a TDP-43-specific antibody (Fig. 5d, e). We visualized tagged intronic lariats by fluorescence microscopy. Remarkably, in every *dbr1*Δ cell analyzed, TDP-43 co-localized with intronic lariats (Fig. 5e). Consistent with our genetic results (Fig. 5a) and fluorescence microscopy experiments (Fig. 5c), TDP-43 was not retained in the nucleus in *dbr1*Δ cells and accumulated in the cytoplasm (Fig. 5e). However, the size and shape of TDP-43 inclusions were profoundly different in *dbr1*Δ and WT cells. In WT cells, TDP-43 formed multiple small, irregular shaped cytoplasmic foci (Fig. 5d), whereas in *dbr1*Δ cells, TDP-43 always formed at least one large, perfectly round focus (Fig. 5d), which always co-localized with intronic lariats (Fig. 5e).

Intronic lariats associate with TDP-43 and compete with other RNAs for binding to TDP-43

We also assessed whether the TDP-43 ribonucleoprotein complex contains lariats by biochemical means. We expressed TDP-43 containing a Flag epitope tag in WT and *dbr1*Δ cells and immunoprecipitated TDP-43 from cell lysates with an anti-Flag antibody. The associated RNA was separated by two-dimensional electrophoresis. Linear RNA molecules migrate in a diagonal on the two-dimensional gels, but lariat and lariat breakdown products migrate in a separate arc owing to the reduced mobility conferred by their altered structure (Supplementary Fig. 6a). As expected, in WT and *dbr1*Δ cells, TDP-43 associated with RNAs. However, in *dbr1*Δ cells, the TDP-43 ribonucleoprotein complex contained additional RNA species, consistent with intronic lariats.

Finally, to directly test our hypothesis that intronic lariats formed in *dbr1*Δ cells act as decoys for TDP-43 by competing with it for binding to other cellular RNAs, we performed *in vitro* electrophoretic mobility shift assays. Incubation of a radioactively labeled RNA

Author Manuscript Author Manuscript Author Manuscript Author Manuscript

probe known to bind TDP-43 (UGAAAAUUAAUGUGUGUGUGUGGAAAAUU)[46] with recombinant TDP-43 results in a gel shift (Supplementary Fig. 6 b, c). We isolated total RNA from WT and *dbr1*Δ cells and tested the ability of these RNAs to compete for binding to TDP-43. As expected, RNAs from WT and *dbr1*Δ cells competed for TDP-43 binding (Supplementary Fig. 6b), consistent with TDP-43 binding a large number of RNA targets[47]. To specifically test the ability of intronic lariats to compete for binding to TDP-43 (i.e., to act as decoys), we treated RNAs isolated from WT and *dbr1*Δ cells with RNase R, which degrades all RNAs except for branched lariats[48]. When these RNase R-treated samples were incubated with the TDP-43 binding reaction, only the RNase R-treated RNAs isolated from *dbr1*Δ cells competed TDP-43 away from its binding site (Supplementary Fig. 6c). Thus, *dbr1*Δ cells contain an RNase R-resistant species, likely intronic lariats, that compete for binding to TDP-43.

DISCUSSION

Using two unbiased genetic screens in yeast, we discovered Dbr1 as a potent modifier of TDP-43 toxicity. We provide evidence that in the absence of Dbr1, intronic lariats accumulate in the cytoplasm, and we propose that these act as decoys to sequester TDP-43 away from interfering with essential RNAs and RNA-binding proteins. Thus, we suggest that the debranching enzymatic activity of Dbr1 could be a novel therapeutic target to combat toxic effects from cytoplasmic TDP-43 aggregation in ALS. The additional genetic modifiers of TDP-43 toxicity uncovered from these two yeast screens (Table 1 and Supplementary Dataset 1) will hopefully provide even more insight into disease mechanisms and open novel avenues for therapeutic intervention.

Recent studies indicate that RNA-binding is an important component of TDP-43 toxicity in cellular and animal models[19,22,49,50]. One potential mechanism of neurotoxicity is that TDP-43 aggregates in the cytoplasm, sequestering essential cellular RNAs and RNA-binding proteins away from their normal function. This could lead to catastrophic changes in RNA metabolism, owing to defects in RNA stability, splicing, transport and/or translation of essential RNAs. This effect might be more deleterious to motor neurons if motor neuron-specific transcripts were preferentially sequestered by TDP-43 or even if motor neurons were simply more sensitive to subtle alterations in any of these RNA metabolic pathways. TDP-43 loss-of-function likely also contributes to disease. TDP-43 is depleted from nuclei of affected neuronal populations in ALS patients[8], and down-regulation of TDP-43 in mouse leads to widespread dysregulation of splicing[47]. Finally, TDP-43 mutations might act in a dominant negative manner, interfering with the function of WT TDP-43[51,52]. These three pathogenic mechanisms (gain-of-toxic properties in the cytoplasm, loss-of-function from the nucleus, and dominant negative effects) are almost certainly not mutually exclusive and likely all contribute to ALS pathogenesis.

Inhibiting Dbr1 function might overcome or prevent cytoplasmic TDP-43 (and FUS/TLS) aggregates from wreaking havoc on critical RNAs and RNA-binding proteins. We propose the accumulated intronic lariat species in *dbr1*Δ cells suppress TDP-43 toxicity by acting as decoys, causing TDP-43 to bind to them rather than to important cellular RNA targets (Fig. 5f). The catalog of genome-wide RNA targets for TDP-43 is emerging[47,53-55]. Intriguingly,

Author Manuscript Author Manuscript Author Manuscript Author Manuscript

TDP-43 appears to preferentially bind to long intronic pre-mRNA sites compared to coding exonic regions or UTRs[47]. This might explain why the intronic RNA sequences (lariats) that accumulate in *dbr1*Δ cells sequester TDP-43 away from other RNA species in the cell and suppress TDP-43 toxicity. TDP-43 might also preferentially recognize the lariat branch point structure or binding to the lariat promotes nucleation or other alterations to TDP-43 conformation.

For Dbr1 to be a therapeutic target, several questions must be addressed. Wouldn't inhibition of Dbr1 debranching activity be toxic itself? Indeed, the highest concentration of Dbr1 siRNA (50 nM) in primary rat neurons increased the risk of death (Supplementary Fig. 3), suggesting too much Dbr1 inhibition could be deleterious. However, in budding yeast, Dbr1 deletion is tolerated (Fig. 1a), and siRNA knockdown in M17 cells does not result in growth inhibition (M.A. and A.D.G. unpublished and[56]). Nevertheless, it will be important to determine what level of Dbr1 inhibition is tolerated and if an appropriate therapeutic index can be achieved. An additional consideration for this approach in mammalian cells is the non-coding RNAs in intronic regions that depend on Dbr1 activity. Expression of these non-coding RNAs may be dysregulated by Dbr1 inhibition, and the consequences of this must be assessed. Furthermore, since abnormal accumulation of RNA is hypothesized to trigger autoimmunity and there would likely be a large pool of lariats in human cells, the effects of Dbr1 inhibition on autoimmuity should be analyzed. Although, to our knowledge, Dbr1 inhibitors are not available, our novel method to visualize intronic lariats in living cells (Fig. 4) will facilitate screening of chemical compound libraries for small molecule Dbr1 inhibitors.

There are currently no TDP-43-directed therapies for ALS or related TDP-43 proteinopathies. Antisense oligonucleotides and RNA interference approaches are emerging as attractive therapeutic strategies in neurodegenerative diseases in which decreasing levels of a toxic mutant protein might be efficacious[57–60]. Indeed, treating a mouse model of inherited ALS (caused by a mutation in SOD1) with antisense oligonucleotides to SOD1 significantly slowed disease progression[4]. This approach offers tremendous promise for treating ALS patients with SOD1 mutations, but since mutations in SOD1 account for only ~2–5% of all ALS cases, additional therapeutic strategies are needed. Because TDP-43 appears to contribute to ALS pathogenesis broadly[7], targeting TDP-43 with antisense approaches could be effective. However, it is unknown if TDP-43 contributes to disease via loss- or gain-of-function mechanisms[61], mandating caution in pursuing TDP-43-lowering approaches. We present an alternative strategy: by targeting Dbr1, by small-molecule inhibitors or antisense oligonucleotides, it might be possible to antagonize TDP-43's toxic effects in the cytoplasm, without interfering with potential critical functions in the nucleus.

ONLINE METHODS

Yeast strains, media, and plasmids

The *dbr1*Δ strain was obtained by replacing the *DBR1* coding region with a KanMX4 cassette in the BY4741 or W303 strains and verified by colony PCR. CEN and 2-micron galactose-inducible TDP-43[28], 2-micron ΔNLS-TDP-43-YFP[22], FUS[21], α-synuclein[62], and Htt103Q expression plasmids were as described[63].The yeast Dbr1 mutant expression

Author Manuscript Author Manuscript Author Manuscript Author Manuscript

plasmids [33] and m-TAG plasmids pLOXHIS5MS2L, pSH47 and pMS2-CP-GFP (x3) were as described [44].

Yeast TDP-43 toxicity modifier screens

We used the synthetic genetic array (SGA) technique to screen the collection of non-essential only (Screen 1, performed in A.D.G. laboratory) yeast knockout strains or a collection of non-essential yeast knockout strains combined with essential genes reduced in expression by DAmP[27] (Screen 2, performed in the laboratories of R.V.F. and N.K.) for modifiers of TDP-43 toxicity. These screens were performed as described[26,64,65] with some modifications[66], using a Singer RoToR HDA (Singer Instruments, Somerset, UK). For screen 1, the galactose-inducible TDP-43 expression construct (pAG416Gal-TDP-43) was introduced into MATα strain Y7092 to generate the query strain. This query strain was mated to the yeast haploid deletion collection of non-essential genes (MATa, each gene deleted with KanMX cassette; Fig. 1A). Haploid mutants harboring the TDP-43 expression plasmid were grown in the presence of glucose (TDP-43 expression "off") or galactose (TDP-43 expression "on"). After growth at 30°C for 2 days, plates were photographed and colony sizes measured by ImageJ image analysis software, based on[67]. The entire screen was repeated three times and only hits that reproduced all three times were selected for further validation by random spore analysis on DNA sequencing of deletion strain bar codes.

For screen 2, a control query strain containing the empty vector was generated by transforming the yeast strain BY5563 (Mat α) with p415 Gal GFP and the experimental query strain was generated by transforming BY5563 (Mat α) with p415 Gal TDP-43-GFP. Both strains were mated with the combined yeast knockout-DAmP collection (Mat a) and haploid yeast containing the deletion/DAmP yeast gene with the control or experimental plasmid were selected as described[65]. Three biological replicates were isolated by selecting for haploid yeast after sporulation on three plates. Each biological replicate was duplicated to generate six replicates (three biological and two technical replicates per biological replicate). Plates were imaged at several time points after final inoculation on glucose or galactose. Colony size was assessed as described[67].

Isolation and culturing of primary cortical neurons

Rat cortical neurons were isolated from embryonic d20–21 rat (Sprague Dawley) pups, cultured in serum-free media in 96 well plates for 4 days *in vitro*, and then transfected using Lipofectamine2000 (Invitrogen; full protocols at http://www.gladstone.ucsf.edu/gladstone/site/finkbeiner/). Neurons were transfected with plasmids (pGW1 backbone) encoding mApple and either TDP-43-EGFP or EGFP, and with siRNA (SMARTpool, Dharmacon) directed against DBR1 or scrambled siRNA.

Live cell imaging for longitudinal analysis

For neuronal survival analysis, we used a robotic imaging system as described[68,69]. Briefly, approximately 24–48 hours after transfection, images were obtained with an inverted Nikon microscope (TE2000) equipped with PerfectFocus, an extra-long working distance (ELWD) 20× objective lens, and an Andor Clara 16-bit, ultra-cooled camera. Illumination was provided by an adjustable, high-intensity, and long-lasting xenon lamp and a liquid light

Author Manuscript Author Manuscript Author Manuscript Author Manuscript

guide to maximize the signal-noise ratio. The stage and shutter movements, fluorescence excitation and emission filters, focusing, and imaging acquisition are fully automated and controlled through a 64-bit host computer running a combination of proprietary software (ImagePro, Media Cybernetics) and custom-designed algorithms.

Survival analysis

Digitized images from the RFP (mApple) and GFP (TDP-43-EGFP) channels were assembled into montages with ImagePro (Media Cybernetics), and cells were prospectively counted in the RFP channel by original code developed in MatLab. Cell death was marked by loss of fluorescence, membrane rupture, or neurite retraction. The time of death for each neuron was determined by the last time that the neuron was seen. Kaplan-Meier and cumulative risk of death curves were generated using the survival package in R. Statistical significance of survival differences between cohorts of neurons was determined by the log-rank test, and Cox proportional hazards analysis was used to measure the relative change in the risk of death, or hazard ratio.

Two-dimensional nucleic acid gels

Nucleic acid pellets from immunoprecipitation were resuspended in 5 μl of DEPC water and 5 μl of 2X nucleic acid loading dye (0.025 g xylene cyanol, 0.025 g bromophenol blue in 100% formamide) and heated at 85°C for 5 min. Nucleic acids were separated in the first dimension by loading samples into a prerun (300 V for 10 min) 5% polyacrylamide gel (19:1, acrylamide:bis-acrylamide) containing 7 M urea and 1X TBE (90 mM Tris base, 90 mM boric acid, 2 mM EDTA, pH 8.0) and electrophoresing samples at 300 V. Nucleic acids were separated in the second dimension by placing the entire lane from the first dimension gel above the second dimension gel. Second dimension gel was exactly the same as the first dimension gel except the polyacrylamide percentage is 10%. Samples were electrophoresed at 300 V until xylene cyanol dye reached the bottom of the second dimension gel. Two-dimensional nucleic gels were washed briefly in water and then placed in 1X Sybr Gold (Invitrogen) solution prepared in water. Gels were protected from light and gently agitated at 23–25°C in 1X Sybr Gold solution for 45 min. Images of the gel were captured on an ultraviolet light box at an excitation wavelength of 302 nm and a 4-sec exposure time.

Genomic tagging strategy to visualize intronic lariats

To visualize intronic lariats in *dbr1*Δ cells, we adapted the m-TAG protocol[42] for use with introns. We used PCR-based chromosomal gene tagging, using homologous recombination to integrate the *loxP::Sphis5+::loxP::MS2L* cassette into the intron of either the *ACT1* gene or the *CYH2* gene in WT or *dbr1*Δ cells. For *ACT1*, we inserted the MS2L cassette at bp 159 of the *ACT1* genomic DNA sequence (ACT1/YFL039C on chromosome VI from coordinates 54696 to 53260). For *CYH2*, we inserted the MS2L cassette at bp 303 of the *CYH2* genomic DNA sequence (RPL28/YGL103W on chromosome VII from coordinates 310967 to 311927). To excise the loxP-flanked *Sphis5* cassette, we transformed cells with plasmid pSH47, which expresses Cre recombinase under control of the galactose-regulated promoter. Proper integration of MS2L sequences was verified by colony PCR and DNA sequencing.

Author Manuscript Author Manuscript Author Manuscript Author Manuscript

Visualizing tagged intronic lariats by fluorescence microscopy

We visualized MS2-tagged intronic lariats in WT and *dbr1*Δ cells as described in[42]. We transformed WT and *dbr1*Δ cells, harboring an MS2-tagged *ACT1* intron, with pMS2-CP-GFP(x3), which expresses MS2-CP fused to three copies of GFP under the control of the *MET25* promoter. Yeast cells were fixed with 70% ethanol and stained with DAPI in Vectashield mountaing medium. Colocalization of an *MS2L*-tagged intronic lariat with TDP-43 was determined using fluorescence microscopy to detect lariats (GFP) and immunocytochemistry with a TDP-43-specific antibody to detect untagged TDP-43.

TDP-43 lentiviruses

To generate a lentiviral vector for the conditional expression of TDP-43 Q331K, an N-terminally FLAG- and C-terminally myc-tagged TDP-43Q331K Gateway entry clone was used in a Gateway LR reaction to transfer it to the pSLIK-Neo lentiviral destination vector. Recombinant lentiviruses were produced as described in[70]. For lentiviral transduction, human M17 neuroblastoma cells (ATCC) were incubated with lentiviral supernatants for 6 h at 37°C. Stable cell lines were selected by culturing transduced cells for 5 days in growth medium (minimum essential medium (MEM) alpha /F-12 (Invitrogen) containing 10% heat-inactivated fetal bovine serum, 100 U/ml penicillin, and 100 μg/ml streptomycin (complete medium) with 100 μg/ml Geneticin). Individual clones were selected and analyzed for inducible expression by immunoblotting and immunofluorescence analysis.

TDP-43 toxicity assay in mammalian cells

We assessed the effect of TDP-43 on cell proliferation in the MTT assay. M17 cells stably transduced with either an empty vector or with the TDP-43 Q331K vector were seeded in 96-well plates. To induce TDP-43Q331K expression, doxycycline (0.1, 1, or 2 μg/ml) was added to the growth medium, and cells were incubated for 3 days. To measure proliferation, MTT (3-(4,5-dimethylthiazol-2-yl)-2,5-diphenyltetrazolium bromide) was added to each well and incubated for 4 h at 37°C. Acidic isoproponal (40 mM HCl) was then added to each well to solubilize the blue formazan crystals. Absorbance at 570 nm was read with a Tecan Safire II plate reader. Absorbance measurements were normalized to the absorbance of cells not treated with doxycycline and used to calculate a percent viability for each condition. Two-way ANOVA was used to evaluate differences in means between two groups, and $P < 0.05$ was considered statistically significant. Each condition was replicated at least four times and each experiment was independently repeated at least three times.

siRNA knockdown of Dbr1 in M17 cells

siRNAs targeting human Dbr1 and non-targeting control siRNAs were purchased from Thermoscientific (Dbr1, catalog #J-008290-08-0005; non-targeting, catalog #D-001810-01-05). siRNA knockdown was validated by immunoblotting with a Dbr1-specific antibody (Proteintech, rabbit polyclonal catalog #16019-1-AP). The M17 cell line with inducible TDP-43 Q331K expression was transfected with 50 nM of hDbr1 siRNAs or non-targeting control siRNAs using RNAi Lipofectamine (Invitrogen). Two days later cells were treated with media containing doxycycline (0 and 1 μg/ml) to induce expression of TDP-43 and then toxicity was assessed by MTT assay after 2 days (day 4). TDP-43 toxicity

Author Manuscript Author Manuscript Author Manuscript Author Manuscript

in M17 cells treated with Dbr1 siRNAs was compared to toxicity in cells treated with non-targeting control siRNAs or empty vector.

TDP-43 in vitro RNA-binding assay

GST-TDP-43 was purified from *E. coli* as described[20]. RNA-binding assays were performed as described[71]. Briefly, competitor RNA was purified from WT W303 yeast or *dbr1*Δ W303 yeast using an RNeasy Mini Kit (Qiagen) and was either left untreated or treated with RNase R to degrade any linear RNA structures while leaving lariat RNA intact. After RNase R treatment, RNA was purified using an RNeasy MinElute Cleanup Kit (Qiagen). A radioactively labeled RNA probe, UG_6 (5′-GAAAAUUAAUGUGUGUGUGUGGAAAAUU-3′), which is known to bind TDP-43[46], was generated by T7 polymerase-catalyzed transcription of a DNA template in the presence of ^{32}P-labeled UTP. Standard binding reactions were carried out in 10 μl, with a final concentration of 4 mM $MgCl_2$, 25 mM phosphocreatine, 1.25 mM ATP, 1.3% polyvinyl alcohol, 25 ng of yeast tRNA, 0.8 mg of BSA, 1 mM DTT, 0.1 μl Rnasin (Promega, 40 U/ml), 75 mM KCl, 10 mM Tris, pH 7.5, 0.1 mM EDTA, and 10% glycerol. Binding reactions containing GST-TDP-43 (0.5μM) plus ^{32}P-labeled UG_6 (1 μl) were incubated for 15 min at 30°C in the presence of various dilutions of competitor RNA (0–12.9 μg). After binding, reactions were transferred to ice and heparin was added to a final concentration of 0.5 μg/μl; reactions were analyzed on a 4.5% native gel (acrylamide/bis 29:1, BioRad).

Supplementary Material

Refer to Web version on PubMed Central for supplementary material.

Acknowledgments

We thank Kristen Lynch and Sarah Smith for helpful suggestions and discussions about RNA and splicing; Tadashi Nakaya for advice and assistance with lentivirus transduction experiments and analysis; Cornelia Kurischko for advice and assistance with visualizing P-bodies and stress granules; Quinn Mitrovich and Alex Plocik for advice with running the two-dimensional nucleic acid gels; Sean Collins and Dale Cameron for useful advice and assistance in performing the data analysis for screen 2; Brittany Hodges, Divya Hosangadi, Priya Patel, Pierce Nathanson, and Carolin Mrejen for assistance with yeast experiments; Jon Epstein and Alya Raphael for critical comments on the manuscript and helpful suggestions; and Gary Howard for editorial assistance. Andrew Elden helped with initial stages of this project. We are grateful to Dr. Jeffrey Gerst (Weizmann Institute, Israel) for providing the yeast m-TAG plasmids, to Dr. Roy Parker (University of Arizona) for sharing the P-body and stress granule marker plasmids, and to Jimena Weibezahn in Dr. Jonathan Weissman's laboratory (University of California San Francisco) for providing temperature sensitive CDC48 (*cdc48-3*, SM 4783) and wild type CDC48 isogenic (SM 5124) yeast strains. We thank Dr. Beate Schwer for providing the yeast mutant Dbr1 expression plasmids. We thank Dr. Charlie Boone for the MATα strain Y7092. This work was supported by NIH Director's New Innovator Awards 1DP2OD004417 (to A.D.G.) and 1DP2OD002177 (to J.S.), NIH grants NS065317 and NS065317 (to A.D.G.), NS067354 (to J.S.), and GM084448, GM084279, GM081879 and GM098101 (to N.J.K.), a New Scholar in Aging Award from the Ellison Medical Foundation (to J.S.), a grant from the Packard Center for ALS Research at Johns Hopkins (A.D.G. and J.S.), and a grant from the Consortium for Frontotemporal Research (to R.V.F.), NIH grant 2P01AG02074 (to S.F.), a grant from the ALS Association (to S.F.), and the Taube-Koret Center and Hellman Family Foundation (to S.F.). A.D.G. is a Pew Scholar in the Biomedical Sciences, supported by The Pew Charitable Trusts, and a Rita Allen Foundation Scholar. N.J.K. is a Searle Scholar and a Keck Young Investigator. R.V.F. is an Investigator of the Gladstone Institutes. The J. David Gladstone Institutes received support from a National Center for Research Resources Grant RR18928.

Author Manuscript Author Manuscript Author Manuscript Author Manuscript

References

1. Boillee S, Vande Velde C, Cleveland DW. ALS: a disease of motor neurons and their nonneuronal neighbors. Neuron. 2006; 52:39–59. [PubMed: 17015226]
2. Rosen D, et al. Mutations in Cu/Zn superoxide dismutase gene are associated with familial amyotrophic lateral sclerosis. Nature. 1993; 362:59–62. [PubMed: 8446170]
3. Bruijn LI, et al. Aggregation and motor neuron toxicity of an ALS-linked SOD1 mutant independent from wild-type SOD1. Science. 1998; 281:1851–4. [PubMed: 9743498]
4. Smith RA, et al. Antisense oligonucleotide therapy for neurodegenerative disease. J Clin Invest. 2006; 116:2290–6. [PubMed: 16878173]
5. Lagier-Tourenne C, Polymenidou M, Cleveland DW. TDP-43 and FUS/TLS: emerging roles in RNA processing and neurodegeneration. Hum Mol Genet. 2010; 19:R46–64. [PubMed: 20400460]
6. Gitler AD, Shorter J. RNA-binding proteins with prion-like domains in ALS and FTLD-U. Prion. 2011; 5:179–87. [PubMed: 21847013]
7. Mackenzie IR, et al. Pathological TDP-43 distinguishes sporadic amyotrophic lateral sclerosis from amyotrophic lateral sclerosis with SOD1 mutations. Ann Neurol. 2007; 61:427–34. [PubMed: 17469116]
8. Neumann M, et al. Ubiquitinated TDP-43 in frontotemporal lobar degeneration and amyotrophic lateral sclerosis. Science. 2006; 314:130–3. [PubMed: 17023659]
9. Pesiridis GS, Lee VM, Trojanowski JQ. Mutations in TDP-43 link glycine-rich domain functions to amyotrophic lateral sclerosis. Hum Mol Genet. 2009; 18:R156–62. [PubMed: 19808791]
10. Rutherford NJ, et al. Novel mutations in TARDBP (TDP-43) in patients with familial amyotrophic lateral sclerosis. PLoS Genet. 2008; 4:e1000193. [PubMed: 18802454]
11. Sreedharan J, et al. TDP-43 mutations in familial and sporadic amyotrophic lateral sclerosis. Science. 2008; 319:1668–72. [PubMed: 18309045]
12. Van Deerlin VM, et al. TARDBP mutations in amyotrophic lateral sclerosis with TDP-43 neuropathology: a genetic and histopathological analysis. Lancet Neurol. 2008; 7:409–16. [PubMed: 18396105]
13. Yokoseki A, et al. TDP-43 mutation in familial amyotrophic lateral sclerosis. Ann Neurol. 2008; 63:538–42. [PubMed: 18438952]
14. Belzil VV, et al. Mutations in FUS cause FALS and SALS in French and French Canadian populations. Neurology. 2009; 73:1176–9. [PubMed: 19741216]
15. Corrado L, et al. Mutations of FUS gene in sporadic amyotrophic lateral sclerosis. J Med Genet. 2010; 47:190–4. [PubMed: 19861302]
16. Hewitt C, et al. Novel FUS/TLS mutations and pathology in familial and sporadic amyotrophic lateral sclerosis. Arch Neurol. 2010; 67:455–61. [PubMed: 20385912]
17. Kwiatkowski TJ Jr, et al. Science. 2009; 323:1205–8. [PubMed: 19251627]
18. Vance C, et al. Mutations in FUS, an RNA processing protein, cause familial amyotrophic lateral sclerosis type 6. Science. 2009; 323:1208–11. [PubMed: 19251628]
19. Johnson BS, McCaffery JM, Lindquist S, Gitler AD. A yeast TDP-43 proteinopathy model: Exploring the molecular determinants of TDP-43 aggregation and cellular toxicity. Proc Natl Acad Sci U S A. 2008; 105:6439–44. [PubMed: 18434538]
20. Johnson BS, et al. TDP-43 is intrinsically aggregation-prone, and amyotrophic lateral sclerosis-linked mutations accelerate aggregation and increase toxicity. J Biol Chem. 2009; 284:20329–39. [PubMed: 19465477]
21. Sun Z, et al. Molecular determinants and genetic modifiers of aggregation and toxicity for the ALS disease protein FUS/TLS. PLoS Biol. 2011; 9:e1000614. [PubMed: 21541367]
22. Elden AC, et al. Ataxin-2 intermediate-length polyglutamine expansions are associated with increased risk for ALS. Nature. 2010; 466:1069–75. [PubMed: 20740007]
23. Lagier-Tourenne C, Cleveland DW. Neurodegeneration: An expansion in ALS genetics. Nature. 2010; 466:1052–3. [PubMed: 20740002]

Author Manuscript Author Manuscript Author Manuscript Author Manuscript

24. Willingham S, Outeiro TF, DeVit MJ, Lindquist SL, Muchowski PJ. Yeast genes that enhance the toxicity of a mutant huntingtin fragment or alpha-synuclein. Science. 2003; 302:1769–72. [PubMed: 14657499]
25. Giorgini F, Guidetti P, Nguyen Q, Bennett SC, Muchowski PJ. A genomic screen in yeast implicates kynurenine 3-monooxygenase as a therapeutic target for Huntington disease. Nat Genet. 2005; 37:526–31. [PubMed: 15806102]
26. Tong AH, et al. Systematic genetic analysis with ordered arrays of yeast deletion mutants. Science. 2001; 294:2364–8. [PubMed: 11743205]
27. Schuldiner M, et al. Exploration of the function and organization of the yeast early secretory pathway through an epistatic miniarray profile. Cell. 2005; 123:507–19. [PubMed: 16269340]
28. Barmada SJ, et al. Cytoplasmic mislocalization of TDP-43 is toxic to neurons and enhanced by a mutation associated with familial amyotrophic lateral sclerosis. J Neurosci. 2010; 30:639–49. [PubMed: 20071528]
29. Arrasate M, Mitra S, Schweitzer ES, Segal MR, Finkbeiner S. Inclusion body formation reduces levels of mutant huntingtin and the risk of neuronal death. Nature. 2004; 431:805–10. [PubMed: 15483602]
30. Arenas J, Hurwitz J. Purification of a RNA debranching activity from HeLa cells. J Biol Chem. 1987; 262:4274–9. [PubMed: 2435736]
31. Chapman KB, Boeke JD. Isolation and characterization of the gene encoding yeast debranching enzyme. Cell. 1991; 65:483–92. [PubMed: 1850323]
32. Domdey H, et al. Lariat structures are in vivo intermediates in yeast pre-mRNA splicing. Cell. 1984; 39:611–21. [PubMed: 6096014]
33. Khalid MF, Damha MJ, Shuman S, Schwer B. Structure-function analysis of yeast RNA debranching enzyme (Dbr1), a manganese-dependent phosphodiesterase. Nucleic Acids Res. 2005; 33:6349–60. [PubMed: 16275784]
34. Franks TM, Singh G, Lykke-Andersen J. Upf1 ATPase-dependent mRNP disassembly is required for completion of nonsense- mediated mRNA decay. Cell. 2010; 143:938–50. [PubMed: 21145460]
35. Gatfield D, Izaurralde E. Nonsense-mediated messenger RNA decay is initiated by endonucleolytic cleavage in Drosophila. Nature. 2004; 429:575–8. [PubMed: 15175755]
36. Lejeune F, Li X, Maquat LE. Nonsense-mediated mRNA decay in mammalian cells involves decapping, deadenylating, and exonucleolytic activities. Mol Cell. 2003; 12:675–87. [PubMed: 14527413]
37. Larimer FW, Hsu CL, Maupin MK, Stevens A. Characterization of the XRN1 gene encoding a 5′-->3′ exoribonuclease: sequence data and analysis of disparate protein and mRNA levels of gene-disrupted yeast cells. Gene. 1992; 120:51–7. [PubMed: 1398123]
38. van Dijk EL, et al. XUTs are a class of Xrn1-sensitive antisense regulatory non-coding RNA in yeast. Nature. 2011; 475:114–7. [PubMed: 21697827]
39. Igaz LM, et al. Dysregulation of the ALS-associated gene TDP-43 leads to neuronal death and degeneration in mice. J Clin Invest. 2011; 121:726–38. [PubMed: 21206091]
40. Zhang YJ, et al. Aberrant cleavage of TDP-43 enhances aggregation and cellular toxicity. Proc Natl Acad Sci U S A. 2009; 106:7607–12. [PubMed: 19383787]
41. Winton MJ, et al. Disturbance of nuclear and cytoplasmic TAR DNA-binding protein (TDP-43) induces disease-like redistribution, sequestration, and aggregate formation. J Biol Chem. 2008; 283:13302–9. [PubMed: 18305110]
42. Haim L, Zipor G, Aronov S, Gerst JE. A genomic integration method to visualize localization of endogenous mRNAs in living yeast. Nat Methods. 2007; 4:409–12. [PubMed: 17417645]
43. Haim-Vilmovsky L, Gerst JE. m-TAG: a PCR-based genomic integration method to visualize the localization of specific endogenous mRNAs in vivo in yeast. Nat Protoc. 2009; 4:1274–84. [PubMed: 19680241]
44. Haim-Vilmovsky L, Gerst JE. Visualizing endogenous mRNAs in living yeast using m-TAG, a PCR-based RNA aptamer integration method, and fluorescence microscopy. Methods Mol Biol. 2011; 714:237–47. [PubMed: 21431745]

Author Manuscript Author Manuscript Author Manuscript Author Manuscript

45. Mayas RM, Maita H, Semlow DR, Staley JP. Spliceosome discards intermediates via the DEAH box ATPase Prp43p. Proc Natl Acad Sci U S A. 2010; 107:10020–5. [PubMed: 20463285]
46. Buratti E, Baralle FE. Characterization and functional implications of the RNA binding properties of nuclear factor TDP-43, a novel splicing regulator of CFTR exon 9. J Biol Chem. 2001; 276:36337–43. [PubMed: 11470789]
47. Polymenidou M, et al. Long pre-mRNA depletion and RNA missplicing contribute to neuronal vulnerability from loss of TDP-43. Nat Neurosci. 2011; 14:459–68. [PubMed: 21358643]
48. Suzuki H, et al. Characterization of RNase R-digested cellular RNA source that consists of lariat and circular RNAs from pre-mRNA splicing. Nucleic Acids Res. 2006; 34:e63. [PubMed: 16682442]
49. Voigt A, et al. TDP-43-mediated neuron loss in vivo requires RNA-binding activity. PLoS One. 2010; 5:e12247. [PubMed: 20806063]
50. Li Y, et al. A Drosophila model for TDP-43 proteinopathy. Proc Natl Acad Sci U S A. 2010; 107:3169–74. [PubMed: 20133767]
51. Yang C, et al. The C-terminal TDP-43 fragments have a high aggregation propensity and harm neurons by a dominant-negative mechanism. PLoS One. 2010; 5:e15878. [PubMed: 21209826]
52. Estes PS, et al. Wild-type and A315T mutant TDP-43 exert differential neurotoxicity in a Drosophila model of ALS. Hum Mol Genet. 2011; 20:2308–21. [PubMed: 21441568]
53. Sephton CF, et al. Identification of neuronal RNA targets of TDP-43-containing ribonucleoprotein complexes. J Biol Chem. 2011; 286:1204–15. [PubMed: 21051541]
54. Tollervey JR, et al. Characterizing the RNA targets and position-dependent splicing regulation by TDP-43. Nat Neurosci. 2011; 14:452–8. [PubMed: 21358640]
55. Xiao S, et al. RNA targets of TDP-43 identified by UV-CLIP are deregulated in ALS. Mol Cell Neurosci. 2011; 47:167–80. [PubMed: 21421050]
56. Ye Y, De Leon J, Yokoyama N, Naidu Y, Camerini D. DBR1 siRNA inhibition of HIV-1 replication. Retrovirology. 2005; 2:63. [PubMed: 16232320]
57. Xia H, Mao Q, Paulson HL, Davidson BL. siRNA-mediated gene silencing in vitro and in vivo. Nat Biotechnol. 2002; 20:1006–10. [PubMed: 12244328]
58. Xia H, et al. RNAi suppresses polyglutamine-induced neurodegeneration in a model of spinocerebellar ataxia. Nat Med. 2004; 10:816–20. [PubMed: 15235598]
59. Singer O, et al. Targeting BACE1 with siRNAs ameliorates Alzheimer disease neuropathology in a transgenic model. Nat Neurosci. 2005; 8:1343–9. [PubMed: 16136043]
60. Kordasiewicz HB, et al. Sustained Therapeutic Reversal of Huntington's Disease by Transient Repression of Huntingtin Synthesis. Neuron. 2012; 74:1031–44. [PubMed: 22726834]
61. Da Cruz S, Cleveland DW. Understanding the role of TDP-43 and FUS/TLS in ALS and beyond. Curr Opin Neurobiol. 2011; 21:904–19. [PubMed: 21813273]
62. Cooper AA, et al. Alpha-synuclein blocks ER-Golgi traffic and Rab1 rescues neuron loss in Parkinson's models. Science. 2006; 313:324–8. [PubMed: 16794039]
63. Duennwald ML, Lindquist S. Impaired ERAD and ER stress are early and specific events in polyglutamine toxicity. Genes Dev. 2008; 22:3308–19. [PubMed: 19015277]
64. Tong AH, et al. Global mapping of the yeast genetic interaction network. Science. 2004; 303:808–13. [PubMed: 14764870]
65. Tong AH, Boone C. Synthetic genetic array analysis in Saccharomyces cerevisiae. Methods Mol Biol. 2006; 313:171–92. [PubMed: 16118434]
66. Armakola M, Hart MP, Gitler AD. TDP-43 toxicity in yeast. Methods. 2011; 53:238–45. [PubMed: 21115123]
67. Collins SR, Schuldiner M, Krogan NJ, Weissman JS. A strategy for extracting and analyzing large-scale quantitative epistatic interaction data. Genome Biol. 2006; 7:R63. [PubMed: 16859555]
68. Sharma P, Ando DM, Daub A, Kaye JA, Finkbeiner S. High-throughput screening in primary neurons. Methods Enzymol. 2012; 506:331–60. [PubMed: 22341232]
69. Arrasate M, Finkbeiner S. Automated microscope system for determining factors that predict neuronal fate. Proc Natl Acad Sci U S A. 2005; 102:3840–5. [PubMed: 15738408]

Author Manuscript Author Manuscript Author Manuscript Author Manuscript

70. Shinbo Y, et al. Proper SUMO-1 conjugation is essential to DJ-1 to exert its full activities. Cell Death Differ. 2006/1; 13:96–108. [PubMed: 15976810]

71. Rothrock CR, House AE, Lynch KW. HnRNP L represses exon splicing via a regulated exonic splicing silencer. EMBO J. 2005; 24:2792–802. [PubMed: 16001081]

Author Manuscript Author Manuscript Author Manuscript Author Manuscript

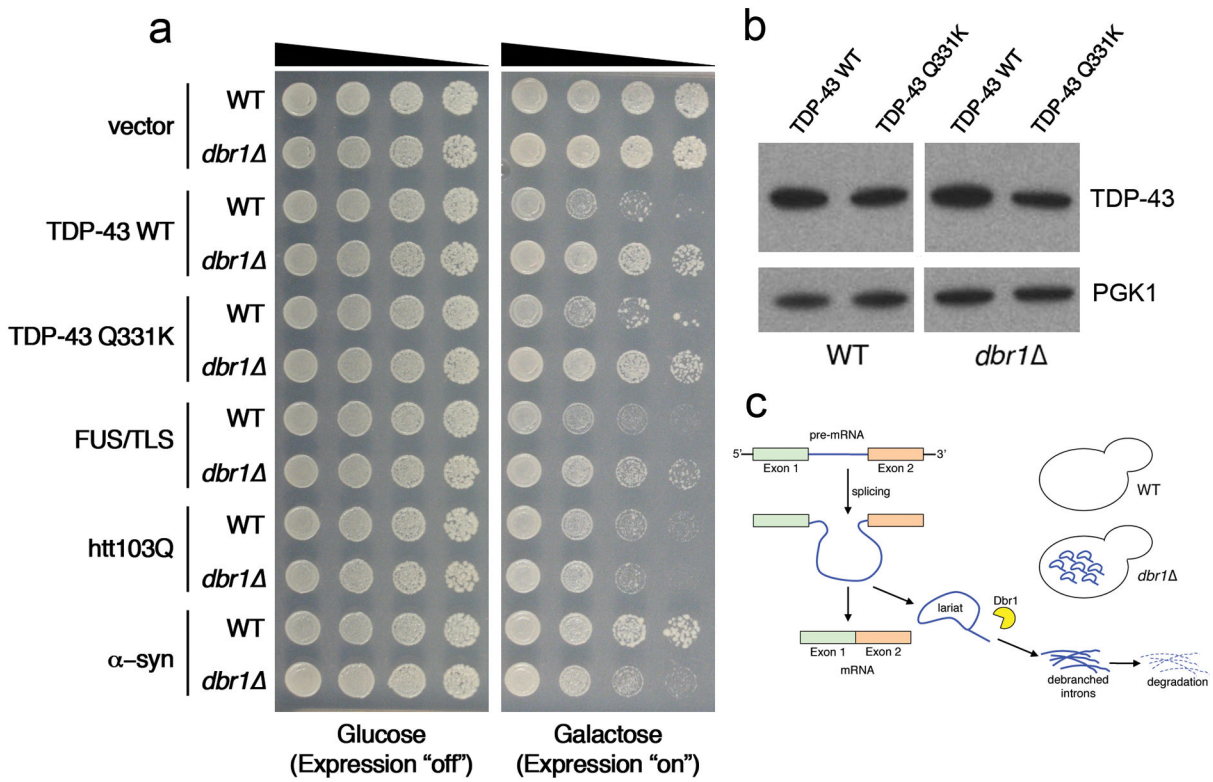

Figure 1.

Dbr1 deletion suppresses TDP-43 toxicity in yeast. **a)** Yeast spotting assays showing that *DBR1* deletion (*dbr1*Δ) suppresses TDP-43 toxicity (WT or ALS-linked Q331K mutant). Fivefold serial dilution of yeast cells spotted onto glucose (TDP-43 "off") or galactose (TDP-43 "on"). **b**) Immunoblotting shows that TDP-43 expression is not affected in *dbr1*Δ cells compared to WT. The effect of toxicity suppression by *dbr1*Δ was specific to ALS-linked RNA binding proteins TDP-43 and FUS/TLS because α-syn or htt103Q toxicity was not suppressed by *dbr1*Δ. Indeed, *dbr1*Δ caused an increase in htt103Q toxicity. **c**) A schematic showing the function of Dbr1 in debranching lariats following splicing. Whereas introns are rapidly degraded in WT cells, in *dbr1*Δ cells intronic lariats accumulate at high levels [33].

Author Manuscript Author Manuscript Author Manuscript Author Manuscript

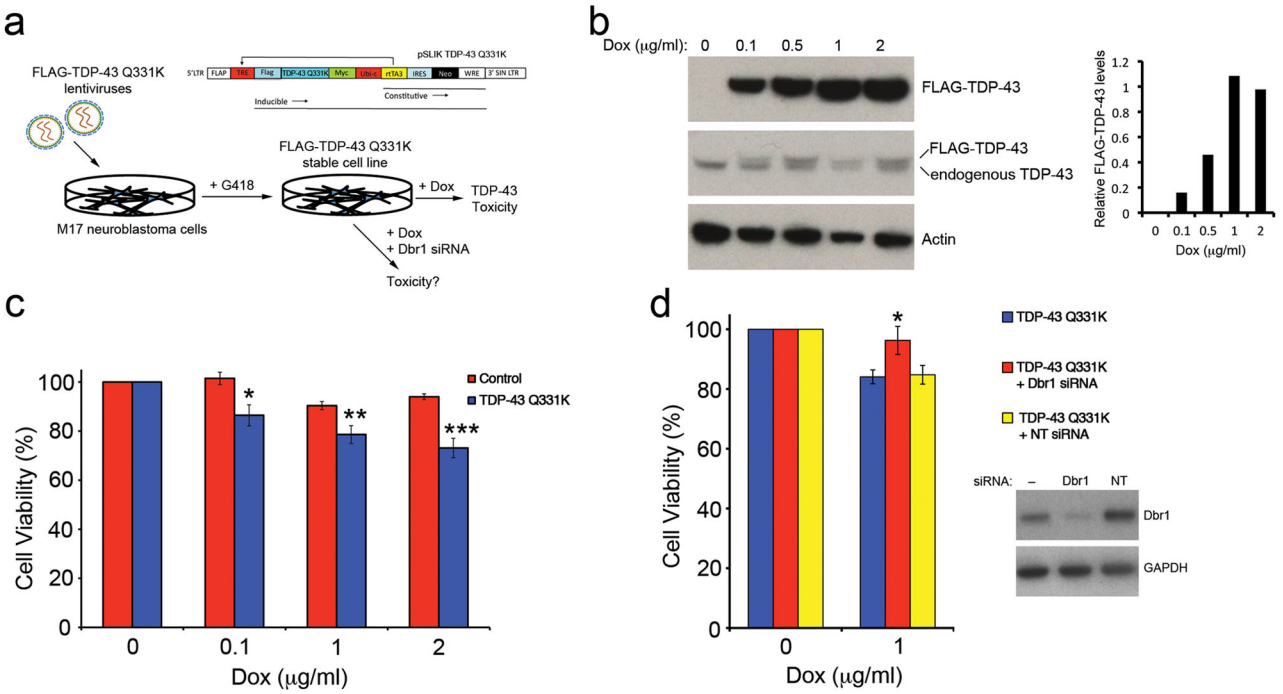

Figure 2.

Dbr1 knockdown reduces TDP-43 toxicity in a human neuronal cell line. **a**) Schematic of approach used to test effect of Dbr1 on TDP-43 toxicity in human cells. Lentiviruses encoding a doxycycline-regulated FLAG-tagged mutant TDP-43 (Q331K) construct were transduced into M17 neuroblastoma cells and stable clones isolated. Addition of doxycycline induced expression of TDP-43 Q331K and resulted in cellular toxicity. Dbr1 expression was knocked down using siRNAs and the effect on TDP-43 toxicity assessed. **b**) Immunoblot showing doxycyline-induced expression of FLAG-tagged TDP-43 Q331K, which migrates slightly slower than the endogenous untagged TDP-43. **c**) Expression of TDP-43 Q331K resulted in decreased cellular viability in a dose-dependent manner compared to control cells (either stably transduced with an empty vector or untransduced), as assessed by the MTT assay (see Methods). * $P < 0.01$, ** $P < 0.05$, *** $P < 0.001$, repeated measures two-way ANOVA. Error bars are mean ± S.E.M. **d**) Cells were transfected with an siRNA against Dbr1 or a non-targeting (NT) siRNA. Immunoblot shows effective knockdown of Dbr1 expression by the Dbr1-specific siRNA but not the non-targeting control siRNA. Untransfected (–) or non-targeting siRNA (NT) transfected cells exhibited decreased viability upon induction of TDP-43 Q331K expression, whereas the Dbr1-specific siRNA increased viability. * $P < 0.05$, repeated measures two-way ANOVA. Error bars are mean ± S.E.M.

Author Manuscript Author Manuscript Author Manuscript Author Manuscript

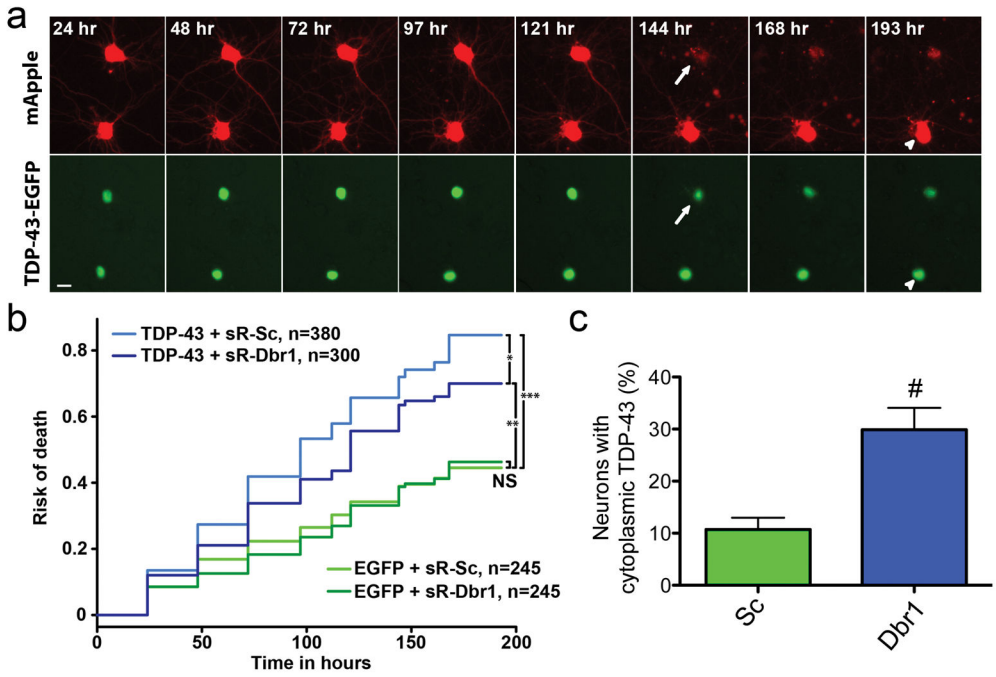

Figure 3.

Dbr1 knockdown reduces TDP-43 toxicity in primary rodent neurons. **a)** Automated fluorescence microscopy of primary rodent cortical neurons transfected with mApple (top row) and TDP-43-EGFP (bottom row). With this system, hundreds of individual neurons are imaged at repeated intervals– two such neurons are depicted here. While one of the neurons lives for the entire experiment (arrowhead), the other neuron has died by 144 hrs (arrow). Scale bar: 10 μm. **b)** Cumulative hazard plot showing the cumulative risk of death for neurons in each cohort as a function of time. Expression of TDP-43-EGFP (light blue curve, n=380 neurons counted) significantly increases the risk of death over that of neurons expressing EGFP alone (light green curve, n=245 neurons counted, HR 2.2). Knockdown of Dbr1 using 30 nM Dbr1 siRNA (sR-Dbr1) in neurons expressing TDP-43-EGFP (dark blue curve, n=300 neurons counted) decreases the risk of death by 19% compared to neurons expressing TDP-43-EGFP that received scrambled siRNA (sR-Sc) (light blue curve, n=380 neurons counted). Data were pooled from 2 independent experiments, and statistical significance determined using Cox proportional hazards analysis. NS, not significant; *** HR 2.23 and $p < 1\times10^{-9}$; ** HR 1.83 and $p < 1\times10^{-4}$; * HR 0.81 and p 0.04. **c)** Using a Kaplan-Meier survival curve to display the same data demonstrates a similar effect on neuron survival. **d)** Dbr1 knockdown results in increased percentage of neurons containing cytoplasmic TDP-43 compared to control scrambled (Sc) siRNA treated neurons. Error bars are mean ± S.E.M. # $p < 0.0005$, two-tailed t test.

Author Manuscript Author Manuscript Author Manuscript Author Manuscript

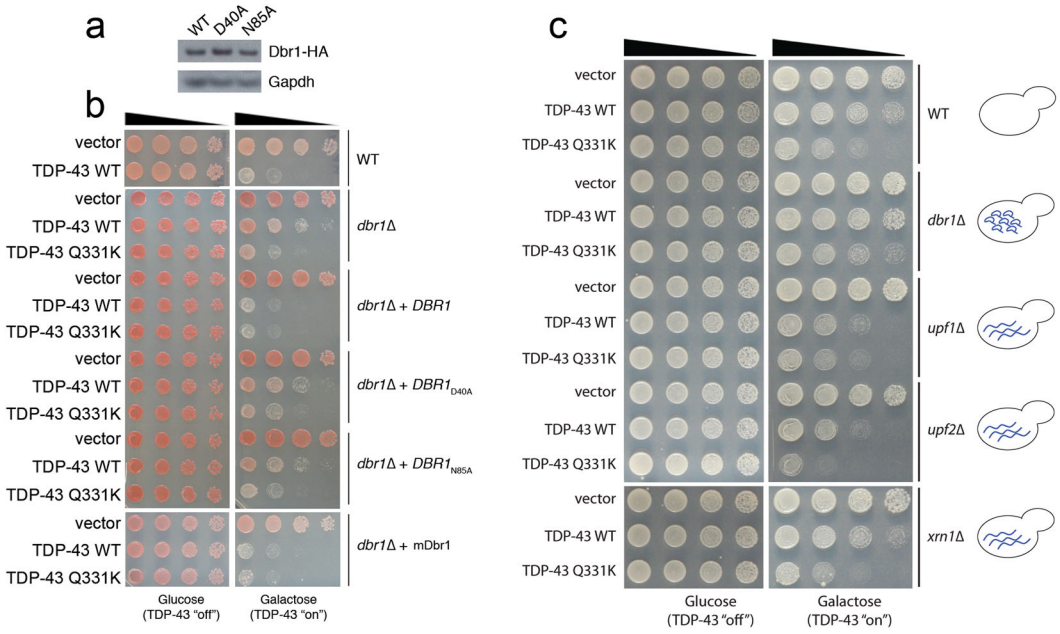

Figure 4.

Dbr1 lariat debranching enzymatic activity is required for TDP-43 toxicity and TDP-43 toxicity suppression is mediated by lariat intron accumulation. **a**) Immunoblot shows that HA-tagged WT Dbr1 and debranching activity dead point mutants [33] are expressed at similar levels. **b**) Yeast spotting assays shows TDP-43 toxicity is suppressed in *dbr1*Δ cells. Expressing WT *DBR1* in *dbr1*Δ cells restored toxicity. Two Dbr1 mutants (D40A or N85A) that lack debranching activity were unable to restore TDP-43 toxicity to *dbr1*Δ cells. Expressing mouse Dbr1 in *dbr1*Δ yeast cells restored TDP-43 toxicity, indicating that the function of Dbr1 is conserved from yeast to mammals. **c**) Yeast spotting assay shows that TDP-43 toxicity is suppressed in *dbr1*Δ cells but not in three other deletion strains (*upf1*Δ, *upf2*Δ, and *xrn1*Δ), which each accumulate non-specific RNA species owing to defects in the cellular nonsense mediated decay (NMD) pathway. Schematic of yeast cells accumulating no excess RNA species (WT), lariat RNAs (*dbr1*Δ) or non-specific linear RNAs (*upf1*Δ, *upf2*Δ, or *xrn1*Δ) are shown next to the spotting assays.

Author Manuscript Author Manuscript Author Manuscript Author Manuscript

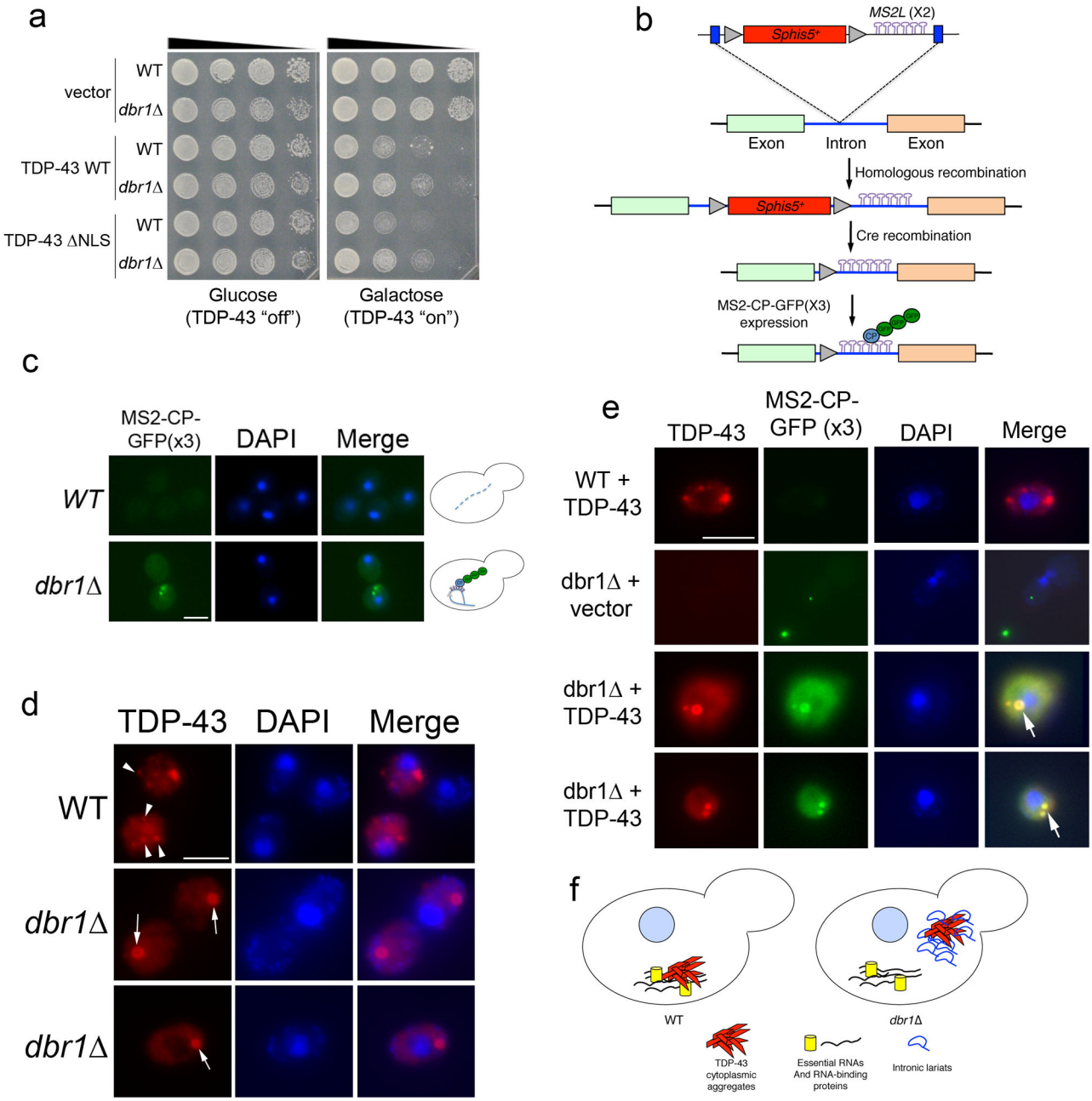

Figure 5.

Intronic lariats colocalize with TDP-43 cytoplasmic foci in yeast. **a**) The toxicity of a TDP-43 mutant (ΔNLS), which is retained in the cytoplasm, is also suppressed by *dbr1*Δ, suggesting that lariat introns are acting in the cytoplasm to suppress toxicity. **b**) Strategy to visualize lariat introns in living cells. Homologous recombination was used to insert an MS2 RNA-binding sequence in the intron of the *ACT1* gene. A GFP-tagged MS2-CP protein was used to visualize accumulated intronic lariats. **c**) In WT cells, lariat introns did not accumulate and the MS2-CP-GFP signal was faint and diffusely localized throughout the cell. In contrast, in *dbr1*Δ cells, MS2-CP-GFP accumulated in one or two bright foci per cell

Author Manuscript Author Manuscript Author Manuscript Author Manuscript

and these were always located in the cytoplasm. Scale bar, 5 μm. **d**) The size and shape of TDP-43 cytoplasmic inclusions was different in *dbr1*Δ cells compared to WT. Whereas in WT cells, TDP-43 formed multiple small irregularly-shaped foci (arrowheads), in *dbr1*Δ cells, there was always at least one large perfectly round focus per cell (arrows) and these always co-localized with lariat introns (see panel e). Scale bar, 5 μm. **e)** Untagged TDP-43 was expressed in WT and *dbr1*Δ cells and visualized by immunocytochemistry with a TDP-43-specific antibody. TDP-43 cytoplasmic foci colocalized with tagged lariat introns (arrows). In addition to the alteration in TDP-43 foci size and shape, the size and shape of the lariat introns also appeared to be altered by the presence of TDP-43 (compare MS2-CP-GFP panel in dbr1Δ+vector and dbr1Δ+TDP-43 cells). Scale bar, 5 μm. **f**) A model of how lariat intron accumulation suppresses TDP-43 cytoplasmic toxicity. In WT cells, TDP-43 aggregates in the cytoplasm and could interfere, via RNA-binding, with essential RNAs and RNA-binding proteins. When Dbr1 activity is inhibited (e.g. in *dbr1*Δ cells), lariat introns accumulate in the cytoplasm and might act as decoys, sequestering TDP-43 away from interfering with important cellular RNAs.

Author Manuscript

Author Manuscript

Author Manuscript

Author Manuscript

Table 1

Yeast gene deletions that enhance or suppress TDP-43 toxicity.

Yeast Strain	Effect on TDP-43 Toxicity	Function	Human homolog
*fld1*Δ	enhancer	Involved in lipid droplet morphology, number, and size; proposed to be involved in lipid metabolism	Berardinelli-Seip congenital lipodystrophy (BSCL2); seipin
*mrpl39*Δ	enhancer	Mitochondrial ribosomal protein of the large subunit	MRPL33
*msn2*Δ	enhancer	Stress-induced transcriptional activator	None
*nhx1*Δ	enhancer	Vacuolar and endosomal Na+/H+ exchanger involved in pH regulation	SLC9A6
*rpl16b*Δ	enhancer	Component of the large (60S) ribosomal subunit	RPL13A
*tif4631*Δ	enhancer	Translation initiation factor	EIF4G1
*cce1*Δ	suppressor	Mitochondrial cruciform cutting endonuclease, cleaves Holliday junctions formed during recombination of mitochondrial DNA	None
*dbr1*Δ	suppressor	RNA lariat debranching enzyme, involved in intron turnover	DBR1
*dom34*Δ	suppressor	Endoribonuclease involved in no-go mRNA decay	PELO
*pbp1*Δ	suppressor	Involved in P-body-dependent granule assembly; interacts with Pab1p to regulate mRNA polyadenylation	ATXN2
*rpl16a*Δ	suppressor	Component of the large (60S) ribosomal subunit	RPL13A
*set3*Δ	suppressor	member of histone deacetylase complex	ASH1
*siw14*Δ	suppressor	Tyrosine phosphatase involved in actin filament organization and endocytosis	None
*ydr067c*Δ	suppressor	Cytoplasmic protein required for replication of Brome mosaic virus in S. cerevisiae, which is a model system for studying replication of positive-strand RNA viruses in their natural hosts	None